Quality Analysis of Antenna Reflection Coefficient in Massive MIMO Antenna Array Module

Marko E. Leinonen, Nuutti Tervo, Marko Sonkki, Aarno Pärssinen
University of Oulu, Oulu, Finland
email: {marko.e.leinonen, nuutti.tervo, marko.sonkki, aarno.parssinen}@oulu.fi

***Abstract*—Number of antennas per an antenna module will increase in upcoming 5G millimeter wave (mmW) radio products. The usage of antenna arrays compensates the increased propagation loss of a radio signal at mmW frequencies. The worst performing antenna defines the quality level MIMO antenna module. This paper presents an analysis and a relationship between the variation of the antenna resonance frequency and the reflection coefficient. A probability density function (PDF) of the antenna reflection coefficient at the specification limit is a non-linearly scaled mirrored version of the PDF of the variation of the antenna resonance. We measured the PDF of antenna reflection coefficient from manufactured prototypes and there is a good correlation between the measured and the simulated PDFs.**

***Index Terms*—Antenna, Impedance matching, mmW, Probability density function, Process capability index, 5G.**

I. INTRODUCITION

One of the drivers for the next generation wireless communication system, 5G, is to increase the data rate up to 10–times higher compared with the current LTE (Long-Term Evolution). Wider signal bandwidths from 100 MHz up to 1 GHz will be needed to support this. The mmW spectrum at the Ka–band (26.5 – 40 GHz) can support the 5G signal bandwidths and the first 5G mmW systems will be deployed at this frequency band [1]. The propagation loss at mmW frequencies is significantly higher compared with the LTE frequencies due to the decreased aperture of a single antenna element. Large antenna arrays can maintain the aperture, but directive beams require active arrays for controlling the beam direction. One of the first 5G Proof-of-Concept (PoC) for a wireless backhaul was demonstrated in the 2018 Winter Olympic Games in Korea, which was developed in 5GChampion EU-project [2]. The massive MIMO (Multiple Input Multiple Output) antenna array of the aforementioned PoC system includes 64 antenna elements and 16 antenna ports and two antenna modules are used in each radio unit [3].

Future 5G mobile terminals and base stations will use even larger antenna arrays than the current PoC systems [1],[4]. Such 5G antenna modules will be more complex to manufacture and production testing will consume more time compared to the LTE antenna modules. Furthermore, high number of antenna elements within the module increases probability of failure and potentially decreases quality level compared with the individual antenna. Thus, the quality level of the antenna module is as good as the quality level of the worst antenna element.

A simplified development process chart of the antenna design is shown in Fig. 1. Specifications of the antenna can be derived from radio regulatory requirements, open standards and product requirements. The antenna impedance matching is an important parameter in the interface specification, especially with RF architectures without a circulator, which stabilizes the antenna impedance seen by a power amplifier [5].

Minimization of a manufacturing failure rate (MFR) is one of the most important tasks for research and development (R&D) perspective during the antenna development process. High quality level increases manufacturing throughput and lowers total unit cost by avoiding rework or scraping costs of defective units. The MFR minimization can be done by minimizing sources of variation in the design, by developing stabile and reliable manufacturing process and by selecting appropriate limits for the manufacturing testing. The testing limits include production variation margins for each antenna parameter. Typically, antennas are 100% conductively tested at the production line for the quality assurance purposes.

II. VARIATION OF ANTENNA REFLECTION COEFFICIENT

The antenna impedance or the antenna reflection coefficient is specified over a frequency band, which is limited by a lower specification limit (LSL) and an upper specification limit (USL). The specification limit in general may be an internal interface limit, a production testing or approval limit, or a regulatory limit. The antenna reflection coefficient can be measured on a linear or logarithm scale. The logarithmic scale is chosen to be used in this paper. Fig. 2. shows an illustration of the reflection coefficient of an antenna port. As it can be noticed, one main resonance dominates the behavior of the antenna reflection coefficient within the specification limits.

The resonance frequency of the antenna may vary, for example due to position inaccuracies of antenna connectors, manufacturing tolerances of mechanical parts, and movements of objects nearby of the antenna array. Typical mechanical manufacturing and positioning tolerances are in range of 0.10 mm, which is significant compared to a wavelength of the mmW signal. The radio board presented in [6] uses 0.2 mm wide signal traces on printed circuit board (PCB). Misalignment of

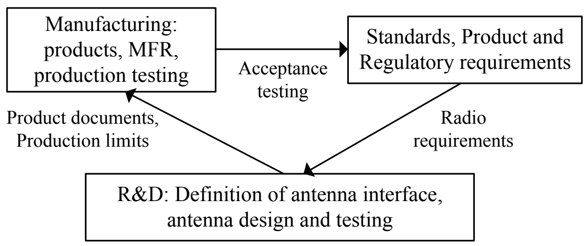

Fig. 1. Development process of the antenna module.

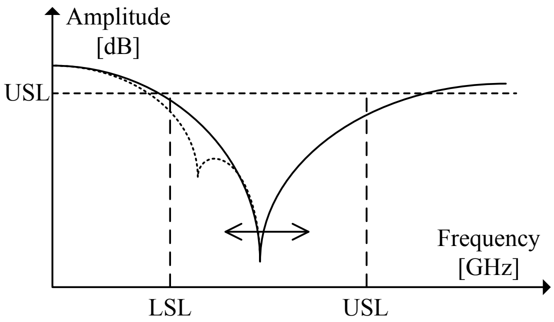

Fig. 2. Resonance notch variation within specification limits.

RF-components to PCB traces may introduce significant variation in the radio performance. The misalignment of the antenna connector or antenna mechanics creates unwanted stray capacitance that changes the impedance matching of the antenna. The change in the impedance matching tunes the resonance frequency of the antenna. A sharp resonance notch is the most sensitive for the impedance change while the reflection coefficient on the other frequency remains relatively constant. Thus, the reflection coefficient curve retains the shape, even if the resonance frequency of the antenna notch varies.

The reflection coefficient at the antenna port varies as a function of the resonance frequency variation, shown in the Fig. 3. The resonance frequency of the antenna varies according to a PDF marked with $f(x)$. A function of the reflection coefficient of the antenna is marked with $g(x)$. Reflection coefficient vary according to distributions $f_{LSL}(x)$ and $f_{USL}(x)$ -values at USL and LSL frequencies and those are a frequency domain mirrored versions of the $f(x)$. The PDFs of the antenna reflection coefficients $h_{LSL}(y)$ and $h_{USL}(y)$ at the specification frequencies can be calculated by mapping the $f_{LSL}(x)$ or $f_{USL}(x)$ with an inverse function of $g(x)$ and scaling it with derivative of inverse function [7]. The PDF of antenna reflection coefficient at LSL frequency $h_{LSL}(y)$ can be then written as

$$h_{LSL}(y) = \begin{cases} f_{LSL}\left(g^{-1}(y)\right)\left|\frac{d}{dy}g^{-1}(y)\right|, & y \in \boldsymbol{Y} \\ 0, & \text{otherwise} \end{cases}, \quad (1)$$

where g^{-1} is the inverse function of $g(x)$ and $\boldsymbol{Y}$ is the set where g^{-1} has continuous derivative. Similarly, the $h_{USL}(y)$ can be calculated by replacing LSL with USL. The PDF of the reflection coefficient at the specification limit frequency is a non-linearly scaled mirrored version of PDF of the variation of the antenna resonance. The inverse function of the $g(x)$ is difficult to calculate for a nonlinear function. The non-linearity of the mapping function transforms the PDF of the antenna reflection coefficient to a long tailed distribution towards small values. Multiple resonances widen the operational frequency band of the antenna, as shown in Fig. 2. If the second resonance is located nearby the specification limit, it may vary over it. This will peak the shape of the distribution of the reflection

TABLE I. PROBABILITY OF DEFECT WITH C_{PK} INDEX

C_{pk} value	0.33	0.66	1.00	1.33	1.50	1.66	2.00
Probability of defect	16.11 %	2.39 %	0.14 %	33.01 ppm	3.40 ppm	0.32 ppm	0.00099 ppm

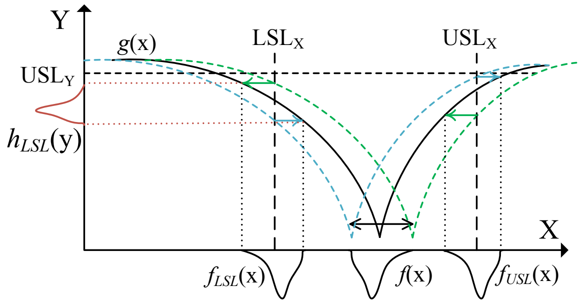

Fig. 3. Relationship between frequency and antenna reflection coefficient variations.

coefficient, because the mapping curve is not a monotonic function. Moreover, there is no a closed form solution for the derivative of the mapping function, if the mapping function $g(x)$ is not a monotonic function.

III. PROCESS CAPABILITY INDEX

Process capability indices (PCI) are widely used in industry to indicate quality level of the technical parameter. PCIs are dimensionless and quality levels of different parameters are comparable to each other. The most widely used PCI is $\boldsymbol{C}_{pk}$ that compares a mean value of the parameter to specification limits of the parameter and it can be calculated [8]

$$\boldsymbol{C}_{pk} = min\left(\frac{USL-\mu}{3\sigma}, \frac{\mu-LSL}{3\sigma}\right), \quad (2)$$

where μ is the mean value of the parameter and σ is the standard deviation of the parameter. The $\boldsymbol{C}_{pk}$ value has a direct mapping to a quality level of the parameter if the parameter follows a normal distribution. A probability of defect can be calculated [8]

$$p_{defect} = 1 - \Phi\left(3\boldsymbol{C}_{pk}\right), \quad (3)$$

where Φ is a cumulative distribution of a standard normal distribution. Summary of probabilities of defects with varied $\boldsymbol{C}_{pk}$ values is shown in Table I. The most commonly used minimum acceptable $\boldsymbol{C}_{pk}$ value for a volume production is 1.33 and the Six Sigma quality methodology recommends value 1.50 [9]. The usage of $\boldsymbol{C}_{pk}$ index with non-normal distributions has been studied in [8],[10]. PCI values may be incorrect or misleading about the product quality, if non-normal data is used with normality-based PCI [10].

TABLE II. QUALITY LEVEL OF MIMO ANTENNA MODULE

# of antennas in the module	C_{pk} level of individual antenna					
	0.66	***1.00***	***1.33***	***1.5***	***1.66***	***2.00***
1	0.66	1.00	**1.33**	1.5	1.66	2.00
2	0.56	0.93	**1.27**	1.45	1.61	1.96
4	0.44	0.85	1.22	**1.40**	1.57	1.92
8	0.31	0.77	1.16	**1.35**	1.52	1.88
16	0.16	0.68	1.09	**1.29**	1.47	1.84
32	-0.03	0.57	1.02	1.23	**1.42**	1.8
64	-0.26	0.46	0.95	1.17	**1.37**	1.76
128	-0.56	0.33	0.88	1.11	**1.31**	1.72
256	-0.96	0.18	0.8	1.04	**1.26**	1.67
512	-1.48	0.00	0.71	0.97	1.20	1.63

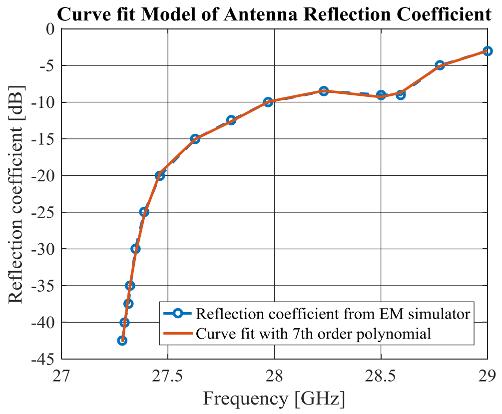

Fig. 4. Model of high side of reflection coefficient curve, $g(x)$.

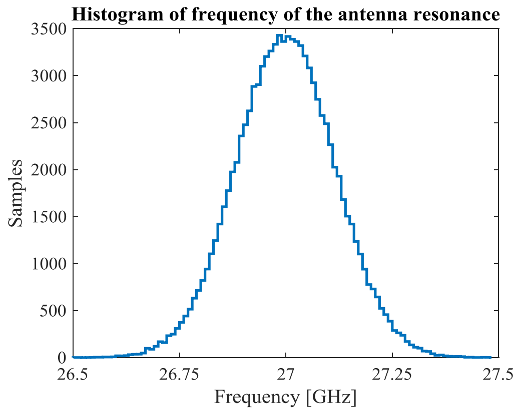

Fig. 5. PDF of the antenna resonace shift, $f(x)$.

The probability of failure of the module can be calculated by multiplying probabilities of good antennas and subtract the result from one as

$$p_{\text{defect}}^{\text{module}} = 1 - \prod_{i=1}^{N} p_{\text{good}}^{i}, \quad (4)$$

where $p_{\text{good}}^{i} = 1 - p_{\text{defect}}^{i}$. The failure probability of the module is converted to corresponding C_{pk} value according to (3). Corresponding C_{pk} values for different size of antenna modules are collected to Table II. As expected, the quality level of the module decreases as the number of antennas per module increases, if the quality level of single antenna is kept fixed. A minimum quality level C_{pk} 1.33 for the antenna module is highlighted in the Table II. The antenna module with 64 elements would require one standard deviation unit stringent design target than the individual antenna to achieve acceptable C_{pk} 1.33. The antenna module including 512 antennas, with individual antenna the quality level C_{pk} 1.0, has C_{pk} value is 0.00 which corresponds failure rate 50% shown table II.

IV. Monte–Carlo Simulation and Verification Measurement Results

A. Single antenna simulations

We verified the shape of the PDF of the antenna reflection coefficient with Monte–Carlo (MC) simulations. Antenna resonance curve shown in Fig 4 is taken from [3], which is based on electro-magnetic (EM) simulation with Finite Element Method of 2 × 1 sub-antenna array. The 2 × 1 sub-array is a subset of the 64–element antenna array [3].

The higher side curve of the main antenna resonance was modelled with a 7th order polynomial, which was the lowest order polynomial to model the shape of the curve smoothly for the MC simulations. The EM simulation indicate that range of notch frequency variation between antenna element resonances is 500 MHz or 1.8% of the center frequency [3]. We used normal distribution to model the variation of the resonance frequency based on our prototype measurement results. The range 500 MHz is assumed equal to ±3 standard deviation (std) units and the mean of the normal distribution is 27.05 GHz and the std is 83.33 MHz. Alternative models are used to model variation of the resonance frequency and lognormal distribution is used in [11].

We performed MC simulations with 100 000 simulation runs. The antenna resonance variation is modelled with PDF shown in Fig. 5 and the result PDF of antenna reflection coefficient at the USL frequency (28.0 GHz) is shown in Fig. 6. A probability plot of simulated PDF of the antenna reflection coefficient is shown in Fig. 7. The MC simulated PDF follows best the 3–parameter Weibull distribution, since it models the best the long tail towards small values. The simulated mean value of the antenna reflection coefficient is −11.664 dB and the std is 1.681 dB. The upper specification limit of the reflection

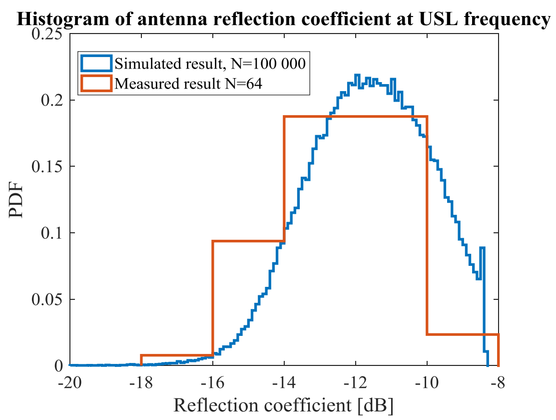

Fig. 6. PDF of the reflection coefficient of one antenna element, $h(y)$.

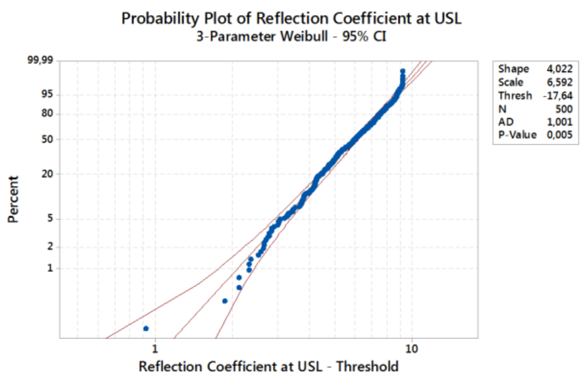

Fig. 7. Weibull distribution test of reflection coefficient PDF of one antenna element, $h(y)$.

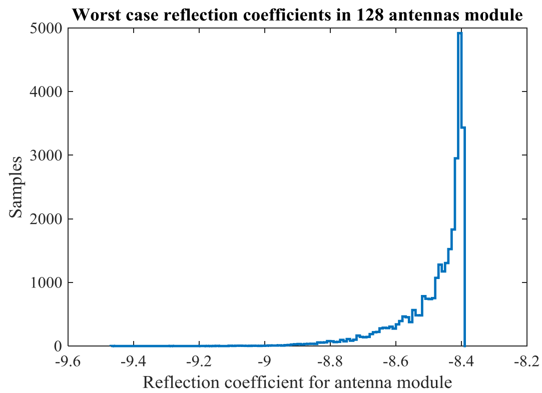

Fig. 8. PDF of maximum reflection coefficient of antenna module of 128 antennas, $h(y)$

coefficient (USL_Y) for the production acceptance limit is −6.0 dB including the production margin. The simulated C_{pk} value is 1.122, but the quality level is under estimated, since all simulated antenna coefficient values are acceptable.

B. *Antenna module simulations*

We performed 30 000 MC simulation runs for antenna modules varying number of antennas in module. Simulations were done with random sampling with replacement based on the data shown in Fig. 6. The maximum individual antenna reflection value or the worst value determines the quality level of the module. The module distribution approaches to the maximum value of reflection coefficient and a peak in Fig. 6 close to maximum value is due to flat mapping function in Fig.4. The number of antennas in the module was varied in simulations from 1 to 256.

The shape of PDF of the maximum reflection coefficient value of the module changes from the lognormal distribution to the normal distribution, when 32 antennas are within the module. As an example, the PDF of the maximum value of antenna reflection coefficient of a 128–antenna module is shown in Fig. 8. The mean value is −8.487 dB, the std is 0.106 dB and the C_{pk} value is 7.849. The C_{pk} value of the antenna module increases from 1.122 to 16.386 when number of antennas increases from 1 to 256 antennas in the module. The improvement of module C_{pk} value is only due to reduction of std of PDF, since the mean value approach to the maximum value of individual antennas. The C_{pk} underestimates the quality level, since none of 30 000 simulated antenna modules exceeded the USL_Y −6.0 dB.

C. *Measurement results from antenna prototypes*

We measured 64 antennas from 4 manufactured antenna modules [3]. The PDF of measured antenna reflection coefficient at high side of the main resonance with simulated one are shown in Fig. 6. The PDF of antenna reflection coefficient is measured at the USL frequency from the notch. The measured PDF follows the 3–parameter Weibull, as well and have a good correlation with the MC simulated PDF. The measured range of frequency variation is 750 MHz which is close to EM simulated 500MHz variation.

V. Conclusions and Future Work

We derived a closed form solution of the PDF of the antenna reflection coefficient when the resonance frequency of the antenna varies with a known PDF. We performed Monte–Carlo simulations to verify the analytical result. The shape of the PDF of the antenna reflection coefficient is a long tailed distribution towards small values. The actual shape of antenna reflection coefficient PDF depends on the steepness of the notch or the impedance matching, the shape and the spread of the PDF of the resonance frequency. We measured antenna reflection coefficients prototype antenna modules, and the shape from the measured PDF matches well with the simulated PDF.

The quality level of massive MIMO antenna array follows the quality level of the worst antenna. Thus, the design target of single antenna element is required to be improved, when number of antenna elements increases in the module since the probability of failure increases accordingly.

Acknowledgment

The research leading to these results has received funding from the European Union H2020 5GPPP under grant n. 723247 and supported by the Institute for Information & communications Technology Promotion (IITP) grant funded by the Korea government (MSIP) (No.B0115-16-0001, 5GCHAMPION). Additionally, this research has been financially supported by Academy of Finland 6Genesis Flagship (grant 318927).

References

[1] F. Boccardi, R. W. Heath, A. Lozano, T. L. Marzetta and P. Popovski, “Five Disruptive Technology Directions for 5G,” *IEEE Commun. Mag.*, vol. 52, no. 2, Feb. 2014, pp. 74–80.

[2] M. Mueck et pal., “5G CHAMPION - Rolling out 5G in 2018,” *IEEE Globecom Workshops*, Dec. 2016, pp. 1–6.

[3] M. Sonkki et al., “Linearly Polarized 64-element Antenna Array for mm-Wave Mobile Backhaul Application,”, in *EUCAP2018,* London, UK, in press.

[4] W. Fan et al., “A Step Toward 5G in 2020: Low-cost OTA performance evaluation of massive MIMO base stations”, *IEEE Antennas and Prop. Mag.*, Feb. 2017, pp. 38-47

[5] A. Prata, S. C. Pires, M. Acar, A. S. R. Oliveira and N. B. Carvalho, "Towards circulator-free multi antenna transmitters for 5G," 2017 *IEEE MTT-S IMS*, Honolulu, HI, 2017, pp. 677-680.

[6] G. Destino et al., “System analysis and design of mmW mobile backhaul transceiver at 28 GHz,” in *EUCNC2017*, Oulu, Finland, 2017, pp. 1–5

[7] G. Casella and R- Berger, *Statistical Inference*. Duxbury press, 1990.

[8] S. Kotz and C. R. Lovelace, “Process Capability Indices in Theory and Practice,” Bristol, UK, Hodder Education Publishers, 1998

[9] F. W. Breyfogle, “Process Capability and Process Performance,” in *Implementing Six Sigma: Smarter Solutions Using Statisical Methods*. New York, NY, USA: Wiley, 1999, pp. 186 – 221.

[10] C.-W. Wu, W. L. Pearn amd S. Kotz,”An Overview of Theory and Practice on Process Capability Indices for Quality Assurance,” Int. J. Prod. Econ., Vol. 117, pp. 338 – 359, 2009

[11] F. Boeykens, H. Rogier and L. Vallozzi, "An Efficient Technique Based on Polynomial Chaos to Model the Uncertainty in the Resonance Frequency of Textile Antennas Due to Bending," in *IEEE Trans. Antennas and Propag.*, vol. 62, no. 3, pp. 1253-1260, March 2014.